

Trapped particle precession and sub-bounce zonal flow dynamics in tokamaks

W. Sengupta^{1,†} and A. B. Hassam¹

¹IREAP, University of Maryland, College Park, USA

(Received 9 September 2017; revised 10 January 2018; accepted 11 January 2018)

A drift-kinetic calculation in an axisymmetric tokamak, with super-diamagnetic flows, is presented to elucidate the relation between the radial electric field, E_r , zonal flows and the rapid precession of the trapped particle (TP) population. It has been shown earlier (Rosenbluth & Hinton, *Phys. Rev. Lett.*, vol. 80(4), 1998, p. 724, hereafter RH) that an initial radial electric field results in geodesic acoustic mode oscillations which subsequently Landau damp, resulting in a much smaller final residual electric field, and accompanying parallel zonal flows. We observe an apparent paradox: the final angular momentum in the RH parallel zonal flow is much smaller than the angular momentum expected from the well-known rapid precession of the trapped particle population in the RH residual electric field. We reconcile this paradox by illuminating the presence of a population of reverse circulating particle flows that, dominantly, are equal and opposite to the rapid TP precession. Mathematically, the calculation is facilitated by transforming to an energy coordinate shifted from conventional by an amount proportional to E_r . We also discuss the well-known RH coefficient in the context of effective mass and show how the TP precession and the opposite circulating flows contribute to this mass. Finally, we show that in the long wavelength limit, the RH flows and RH coefficient arise as a natural consequence of conservation of toroidal angular momentum and the second adiabatic invariant.

Key words: plasma confinement, plasma dynamics, plasma flows

1. Introduction

It is well known that the radial electric field, E_r , plays an important role in tokamak turbulence (Itoh & Itoh 1996; Burrell 1997; Diamond *et al.* 2005; Watanabe, Sugama & Nunami 2011). In particular, shear in E_r can suppress turbulence through generation of zonal flows (Dorland *et al.* 2000; Rogers, Dorland & Kotschenreuther 2000; Terry 2000). Tokamak zonal flows, and the related geodesic acoustic mode (GAM) oscillations, have been widely studied (Itoh *et al.* 2006; Sugama & Watanabe 2006*a,b*, 2009). In particular, an initial radial electric field, $E_r(0)$, in an axisymmetric tokamak results in GAM oscillations. In a collisionless system, the GAMs Landau damp. It has been shown by Rosenbluth and Hinton (RH) (Rosenbluth & Hinton 1998) that, in the asymptotic steady state of this initial value problem, there persists a residual electric field, $E_r(\infty)$, and an associated parallel zonal flow. RH showed

[†]Email address for correspondence: wricksg@gmail.com

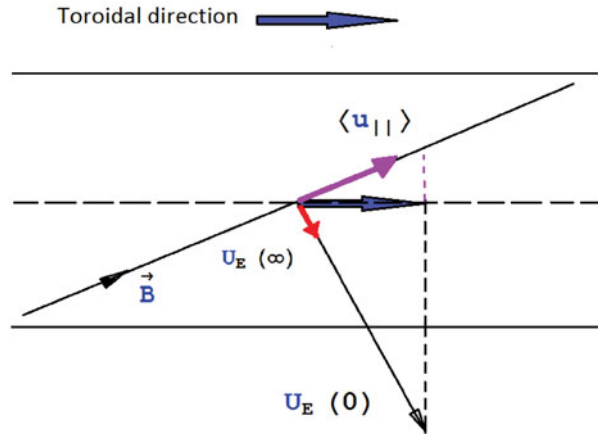


FIGURE 1. Comparison of initial and final RH flows. The initial $\mathbf{E} \times \mathbf{B}$ flow $U_E(0)$, shown in black, reduces to the final $U_E(\infty)$, shown in red. To conserve angular momentum, an average parallel flow $\langle u_{\parallel} \rangle$ must develop, as shown in purple. The field line makes an angle $\approx \epsilon/q$ with the toroidal (horizontal) direction.

that the initial and final electric fields are related according to $E_r(0) = (1 + \mathcal{D})E_r(\infty)$, where $\mathcal{D} \sim 1.6q^2/\sqrt{\epsilon}$ in the large aspect ratio limit. Here, q is the tokamak safety factor and ϵ is the tokamak inverse aspect ratio. Since the initial $\mathbf{E} \times \mathbf{B}$ flow, $U_E(0)$, has a toroidal component and, thus, an initial toroidal angular momentum, and the final $\mathbf{E} \times \mathbf{B}$ flow, $U_E(\infty) \approx (\sqrt{\epsilon}/q^2)U_E(0)$ is much smaller than the initial, a substantial parallel zonal flow must arise in order to preserve angular momentum (see figure 1). The size of the parallel zonal flow, as found by RH, can be deduced from the geometry of figure 1 to be of order $(\epsilon/q)U_E(0)$.

A question arises when one considers the individual contributions to the angular momentum of the trapped particle (TP) and circulating particle (CP) populations of the plasma. It is well known that in the presence of a radial electric field, trapped particles precess toroidally. The speed of precession is of order $(q/\epsilon)U_E$ and represents a rapid rate inasmuch as it is much larger than U_E . In this paper, we note that the angular momentum in the TP population precessing in the final RH electric field is much larger than the total final RH angular momentum. The TP precession angular momentum is of order $\sqrt{\epsilon}(q/\epsilon)U_E(\infty) \approx (1/q)U_E(0)$, while the RH calculated final angular momentum is of order $(\epsilon/q)U_E(0)$, as discussed above. Here we have accounted for the lower density of the trapped fraction, i.e. $n^{\text{TP}} \sim O(\sqrt{\epsilon})$. This represents an apparent paradox: the TP precession is larger than the total angular momentum by a factor of $(1/\epsilon)$.

This line of investigation raises further questions when one calculates separately the CP and TP flows associated with the residual RH zonal flows: as we will show, by direct calculation based on conventional drift-kinetic theory, the RH parallel flow for the TPs is found to be of $O(qU_E(\infty))$, smaller than the precession drift by $1/\epsilon$. In addition, a direct calculation of the net flux surface averaged poloidal flow of the TPs surprisingly gives a non-zero result, namely, a net poloidal flow of $O(qU_E(\infty))$.

As orientation, we note that the RH calculation was done using a gyrokinetic formulation, thus optimally allowing wavelengths of order the ion gyroradius, and allowing $\mathbf{E} \times \mathbf{B}$ flows to be of order the magnetic drifts, \mathbf{v}_D , i.e. $U_E \sim \mathbf{v}_D$. However, as will be shown in this paper, the key results of the RH paper can be checked

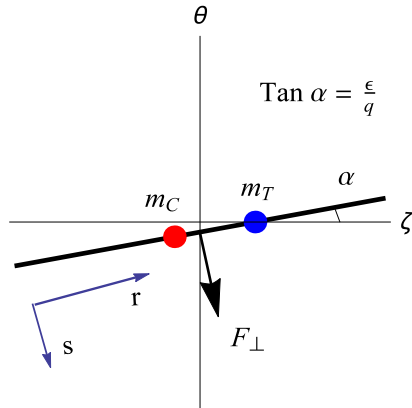


FIGURE 2. Bead-on-wire toy model. The rod models a field line inclined at angle α to the toroidal axis. The rod moves rigidly under force F_{\perp} . Coordinates (r, s) measure distances parallel and perpendicular to \mathbf{B} . A deeply trapped particle (blue) is constrained to move only along the ζ axis. A freely circulating particle (red) moves freely along the rod.

to sustain even in the limit of long wavelengths, or if the super-diamagnetic limit, $U_E \gg v_D$, were taken. Based on this observation, we restrict our calculation in the present paper, right from the start, to long wavelengths and super-diamagnetic flows. Accordingly, we use the drift-kinetic equation of Kulsrud as our starting point. This has the advantage of simplifying the calculations we present, as we will show. Particularly, in the super diamagnetic limit, zonal flows, GAMs and sound waves are decoupled from drift waves and a self-consistent nonlinear analysis of these modes can be carried out completely independent of the complications arising from the drift wave turbulence. Further, since the Kulsrud equations preserve the frozen-in theorem, the underlying physics is simpler to interpret. In particular, frozen-in allows a direct analogy to a bead-on-wire toy model (Cerfon & Freidberg 2011), as we elaborate below.

A toy model can be set-up as follows. We consider a massless rod and two beads of masses m_T, m_C that can slide freely, without interaction, along the rod; one of them (m_T) is further constrained in that it can only move horizontally, that is to say it stays trapped inside a linear horizontal one-dimensional channel. This system is depicted in figure 2. The rod represents a magnetic field line; m_C represents circulating particles, while m_T represents deeply trapped particles. The rod is inclined at a small angle given by $\sin \alpha = \epsilon/q \ll 1$. Consider now an external perpendicular force, F_{\perp} , acting on the rod, as shown in the figure. We define the constrained Newton's equation as $M\dot{s} = F_{\perp}$, where s is the distance measured along F_{\perp} , M is an effective mass and \dot{s} is the speed of the rod in the laboratory frame. The Lagrangian for this system is

$$L(s, \dot{s}, r, \dot{r}) = \frac{1}{2}m_C(\dot{r}^2 + \dot{s}^2) + \frac{1}{2\sin^2 \alpha}m_T\dot{s}^2 + F_{\perp}s, \tag{1.1}$$

leading to the equation of motion,

$$\left. \begin{aligned} \dot{\zeta} &= \frac{\dot{s}}{\sin \alpha} = (q/\epsilon)\dot{s}, & \ddot{s} &= \frac{F_{\perp}}{M}, \\ \text{with } M &= m_C + \frac{m_T}{\sin^2 \alpha} = m_C + m_T \frac{q^2}{\epsilon^2}. \end{aligned} \right\} \tag{1.2}$$

This toy model shows the relative rapid precession of the trapped mass, given by $\dot{\zeta}$. It also shows that the effective mass from the constrained mass, m_T , is $m_T(q^2/\epsilon^2)$.

It follows from the toy model that, inasmuch as the trapped particle precession is rapid and the trapped particle population carries a significant angular momentum, we might expect a corresponding effective mass in the RH problem. When this hypothesis is tested, by adding a torque to the drift-kinetic equations (DKE), an effective mass is indeed identified, and found to be of order $m(1 + \mathcal{D})$. This, however, is much smaller than if the rapid TP momentum was included: this can be shown to give an effective mass of $\sim 1 + O(n^{\text{TP}}q^2/\epsilon^2)$, much larger than the RH effective mass. This heuristic result adds to our original paradox.

Our study in this paper is motivated by an attempt to understand the discrepancy in the individual TP and CP flows and angular momenta, as well as in the naively expected effective mass of the RH problem. The discussion below is organized as follows: In § 2, we present the basic system of equations, consisting of the drift-kinetic equation and the angular momentum conservation equation in axisymmetric toroidal geometry. We then solve the Rosenbluth–Hinton problem in the large flow and long wavelength limit in § 3 and point out the aforementioned discrepancies in the flows. We introduce the shifted coordinates in § 4 and revisit the RH problem in these new coordinates in § 5, to reconcile trapped particle toroidal precession in RH flows. In § 6, we illustrate the role of barely circulating particles in cancelling the large trapped particle precession and thereby explain the smaller overall RH effective mass. Finally, in § 7, we illustrate the role of the second adiabatic invariant in the sub-bounce dynamics of zonal flows. We summarize our results in § 8.

2. Kinetic equations

In this section we present the kinetic equations that are appropriate for studying the physics of the trapped particle precession. We shall only be considering flows that are large compared to the diamagnetic flow and, in principle, can be of the order of poloidal sonic flows. It is then appropriate to use the drift-kinetic equation (DKE) as formulated by Kulsrud (1980). This DKE is derived in the ‘Magnetohydrodynamic (MHD) ordering’ and thus allows large, sonic level $\mathbf{E} \times \mathbf{B}$ flows. In the literature it is also referred to as kinetic MHD (Cerfon & Freidberg 2011; Kunz *et al.* 2015; Burby & Sengupta 2017). Frieman and Hinton-Wong (Frieman, Davidson & Langdon 1966; Hinton & Wong 1985) have obtained equivalent DKEs. A consistent ordering also requires that the parallel electric field E_{\parallel} be very small compared to E_{\perp} . In the electrostatic limit (with frequencies much lower than the Alfvénic frequency) the collisionless DKE is given by

$$\frac{\partial f}{\partial t} + (\mathbf{U}_E + v_{\parallel} \mathbf{b}) \cdot \nabla f + (-\mathbf{b} \cdot ((\mathbf{U}_E + v_{\parallel} \mathbf{b}) \cdot \nabla) \mathbf{U}_E + \mu B \nabla \cdot \mathbf{b} + \frac{e}{M} E_{\parallel}) \frac{\partial f}{\partial v_{\parallel}} = 0, \quad (2.1)$$

where

$$\mathbf{U}_E = \frac{\mathbf{B} \times \nabla \psi}{B^2} \varphi'(\psi), \quad (2.2)$$

is the $\mathbf{E} \times \mathbf{B}$ flow and $f = f(v_{\parallel}, \mu, \mathbf{x}, t)$. The magnetic field \mathbf{B} , in axisymmetry, is given by

$$\mathbf{B} = I \nabla \zeta + \nabla \zeta \times \nabla \psi, \quad \mathbf{B} \times \nabla \psi = I \mathbf{B} - (RB)^2 \nabla \zeta, \quad (2.3a, b)$$

where, R , ζ are the usual radial and toroidal angle in an axisymmetric toroidal geometry and I represents the poloidal current through the flux surface ψ . Here, the E_{\parallel} force term is of the same order as the other parallel force terms (the mirror force and inertial forces) in the equation. The above DKE applies for both ions and electrons, though we will assume small electron mass and thus the electron response will be taken to be adiabatic. The system in the electrostatic approximation consists of four variables, namely, the two distribution functions, the potential φ and E_{\parallel} . The potential φ satisfies the ‘MHD ordering’ $e\varphi/T \approx (1/\rho_*)$, where T is ion/electron temperature and ρ_* is Larmor radius normalized to the system size. These four unknowns are governed by the two DKEs, the quasineutrality condition $n_e = n_i$, and the equation of conservation of angular momentum, namely (Hassam & Kleva 2011)

$$\partial_t \left\langle n\varphi' \frac{|\nabla\psi|^2}{B^2} - \int d^3v \frac{Iv_{\parallel}}{B} f \right\rangle = \tau_{\perp}, \quad \tau_{\perp} = \left\langle n \frac{|\nabla\psi| F_{\perp}}{B m} \right\rangle, \quad (2.4a,b)$$

where $\langle \cdot \rangle$ represents a flux surface average (Helander & Sigmar 2005), and τ_{\perp} is a toroidal torque due to a perpendicular force F_{\perp} . The latter represents an external force, such as from a neutral beam, that could accelerate the $\mathbf{E} \times \mathbf{B}$ flow. It can be shown that in axisymmetric geometry, the equation governing the angular momentum (2.4) is identical to the radial current quasineutrality condition. This equivalence is shown in appendix C. For the present purposes, we will find the former equation to be more convenient. It can also be shown that although the effects of curvature and grad B drifts do not appear in the DKE (2.1), they are fully retained in the current quasineutrality equation (and hence in (2.4)) through the divergence of the Chew–Goldberger–Low (CGL) pressure tensor. This allows us to capture the lowest-order banana width effects that are crucial for the neoclassical shielding effect discussed in RH’s original calculation.

In this paper, we will only be concerned with time scales which are subsonic, i.e. $d/dt \ll c_s/qR$. In this limit, as we will show more precisely later, E_{\parallel} is small and can be neglected. In that case, the system can be closed by simply using the DKE for ions, equation (2.1), and the angular momentum conservation equation (2.4). As a further simplification, we will order $q \gg 1$ but $U_E \sim v_{th}/q$. In this ordering, the nonlinear in U_E terms in the DKE can be neglected compared with cross-terms in v_{\parallel} and U_E , since $|v_{\parallel}U_E \mathbf{b} : \nabla U_E| : |\mathbf{b}U_E : \nabla U_E| \sim 1 : 1/q$. Given these orderings, equation (2.1) can be recast as

$$\frac{\partial f}{\partial t} + (\mathbf{U}_E + v_{\parallel} \hat{\mathbf{b}}) \cdot \nabla f + (v_{\parallel} \mathbf{U}_E \cdot \boldsymbol{\kappa} - \mu \nabla_{\parallel} B) \frac{\partial f}{\partial v_{\parallel}} = 0. \quad (2.5)$$

We now use the form for \mathbf{U}_E , equation (2.2), to simplify (2.5). In particular, $\mathbf{U}_E \cdot \boldsymbol{\kappa} = \mathbf{U}_E \cdot \nabla B/B$, in the low β limit. We also assume axisymmetry and thus $\mathbf{B} \times \nabla \psi \cdot \nabla = IB \nabla_{\parallel}$, where $\nabla_{\parallel} = \mathbf{b} \cdot \nabla$. Given these, (2.5) can be recast to the form

$$\frac{\partial f}{\partial t} + \left(v_{\parallel} + \frac{I\varphi'}{B} \right) \nabla_{\parallel} |_{v_{\parallel}} f + \left(v_{\parallel} \frac{I\varphi'}{B} - \mu B \right) \frac{\nabla_{\parallel} B}{B} \frac{\partial f}{\partial v_{\parallel}} = 0, \quad (2.6)$$

where $f = f(v_{\parallel}, \mu, \mathbf{x}, t)$. We will now use (2.6) and (2.4) as the closed set of equations for the two variables f and φ .

As a closing remark, we reiterate that the large q assumption has been made mainly to simplify the analysis, since it decouples the sound dynamics from the GAM dynamics. A calculation for $q \sim 1$ can be done and has been included in appendix D.

3. Sub-bounce dynamics and the RH problem

In this section, we use (2.4) and (2.6) to study the sub-bounce frequency response of the system. In particular, we will study the zonal flows in response to an externally applied quasi-static force perpendicular to the magnetic field. This approach has the simplification that GAMs are not excited but nevertheless contains all the zonal flow physics that is of interest. We note that RH obtained a sub-bounce response to the gyrokinetic equation, where they self consistently assumed drift ordering, small flows and short perpendicular wavenumber k_{\perp} , such that $k_{\perp}\rho \sim 1$, ρ being the Larmor radius. We will show that the RH zonal flows and the long wavelength RH coefficient Xiao, Catto & Molvig (2007) are obtained self-consistently from our approach.

We perform a linear analysis of the kinetic system (2.4), (2.6) with the electrostatic potential as a small perturbation. We start with an equilibrium, F_0 , with zero flow. From (2.6) we find that the equilibrium distribution function F_0 satisfies

$$v_{\parallel} \nabla_{\parallel} F_0 - \mu \nabla_{\parallel} B \frac{\partial F_0}{\partial v_{\parallel}} = 0, \tag{3.1}$$

which yields $F_0 = F_0(\mathcal{E})$, where $\mathcal{E} = (1/2)v_{\parallel}^2 + \mu B$ is the energy. This F_0 also satisfies the (2.4) with $\tau_{\perp} = 0$. We transform from v_{\parallel} to \mathcal{E} coordinates. The perturbed distribution function, \tilde{f} , satisfies the linearized DKE, which in energy coordinates is given by

$$\frac{\partial \tilde{f}}{\partial t} + v_{\parallel} \nabla_{\parallel} |_{\mathcal{E}} \tilde{f} = v_{\parallel} \nabla_{\parallel} |_{\mathcal{E}} \left(\frac{I\tilde{\varphi}'}{B} v_{\parallel} \right) \frac{\partial F_0}{\partial \mathcal{E}}, \tag{3.2}$$

where $\nabla_{\parallel} |_{\mathcal{E}}$ is the gradient operator at constant \mathcal{E} , and we have used $v_{\parallel} \nabla_{\parallel} |_{\mathcal{E}}(v_{\parallel}) = -\mu \nabla_{\parallel} B$. Since the force is weak, we look for a sub-bounce frequency solution according to the ordering $\partial/\partial t \sim U_E \cdot \nabla \sim F_{\perp} \ll v_{\parallel} \nabla_{\parallel}$. Expanding \tilde{f} as $\tilde{f} = \tilde{f}_0 + \tilde{f}_1 + \dots$ in the smallness of $\partial_t/\omega_b \ll 1$, we obtain, to lowest order,

$$v_{\parallel} \nabla_{\parallel} |_{\mathcal{E}} \tilde{f}_0 = 0 \quad \Rightarrow \quad \tilde{f}_0 = \tilde{f}_0(\mathcal{E}, t). \tag{3.3}$$

To first order, equation (2.6) becomes

$$\frac{\partial \tilde{f}_0}{\partial t} + v_{\parallel} \nabla_{\parallel} |_{\mathcal{E}} \tilde{f}_1 = v_{\parallel} \nabla_{\parallel} |_{\mathcal{E}} \left(I\tilde{\varphi}' \frac{v_{\parallel}}{B} \frac{\partial F_0}{\partial \mathcal{E}} \right). \tag{3.4}$$

Annihilating the \tilde{f}_1 term by bounce averaging (discussed in Helander & Sigmar (2005)), denoted here by overbar as in $\bar{f} = \oint (df/v_{\parallel})/\oint (dl/v_{\parallel})$, we get $\tilde{f}_0 = \bar{f}_0(\mathcal{E})$ which can be set to zero since (3.3) is homogeneous. Solving for \tilde{f}_1 from (3.4) we obtain

$$\tilde{f}_1 = I\tilde{\varphi}' \left(\frac{v_{\parallel}}{B} - g \right) \partial_{\mathcal{E}} F_0, \tag{3.5}$$

where $g(\mathcal{E})$ is yet to be determined and $F'_0 \equiv \partial_{\mathcal{E}} F_0$. To second order we have,

$$\frac{\partial \tilde{f}_1}{\partial t} + v_{\parallel} \nabla_{\parallel} |_{\mathcal{E}} \tilde{f}_2 = 0. \tag{3.6}$$

Annihilation of (3.6) yields $\overline{\partial \tilde{f}_1} = 0$, which gives $g = \overline{(v_{\parallel}/B)}$. Thus, we get the RH solution for \tilde{f}_1 correct to first order (Xiao *et al.* 2007), *viz.*

$$\tilde{f}_1 = I\tilde{\varphi}' \left(\frac{v_{\parallel}}{B} - \overline{\left(\frac{v_{\parallel}}{B} \right)} \right) \partial_{\mathcal{E}} F_0. \tag{3.7}$$

Let us now check for self-consistency of the above calculation, in particular the neglect of E_{\parallel} . We can use \tilde{f}_0 and \tilde{f}_1 above to calculate the density. Since $\tilde{f}_0 = 0$, and the first order \tilde{f}_1 is antisymmetric in v_{\parallel} , density remains constant up to second order. Likewise, changes in parallel and perpendicular pressures are also zero because of parity. The elements of the electron pressure tensor can be used to *a posteriori* calculate E_{\parallel} , as defined in equation (49) of the Kulsrud (1980) manuscript. (For massless electrons, E_{\parallel} is given essentially by the generalized adiabatic electron response, *viz.*, $neE_{\parallel} = -\mathbf{b}\nabla : \mathbf{P}_e$.) We find that $E_{\parallel} = 0$ to lowest order and also zero to first order given the f_1 symmetry. This self-consistently justifies the neglect of E_{\parallel} in our calculation above.

3.1. Rosenbluth–Hinton \parallel flows

We now calculate the parallel flow by taking the v_{\parallel} moment of $\tilde{f} = \tilde{f}_0 + \tilde{f}_1$. Since $\tilde{f}_0 = 0$, we have

$$n_0 \tilde{U}_{\parallel 1} = \int d^3 v v_{\parallel} \tilde{f}_1 = I\tilde{\varphi}' \int d^3 v v_{\parallel} \left(\frac{v_{\parallel}}{B} - \overline{\left(\frac{v_{\parallel}}{B} \right)} \right) \partial_{\mathcal{E}} F_0. \tag{3.8}$$

Until now, we have not done a large aspect ratio expansion. However, to evaluate the integrals and compare the leading-order scaling behaviour of the flows with respect to the trapped precession, we shall now consider the inverse aspect ratio ϵ as a small parameter. The analysis is straightforward and has been presented in detail by several authors (Xiao *et al.* 2007; Sugama & Watanabe 2009). Here we include a few details for completeness.

In the large aspect ratio circular flux surface limit with $B = B_0(1 - \epsilon \cos \theta)$, θ being the poloidal angle, we find that

$$\overline{\left(\frac{v_{\parallel}}{B} \right)} = \frac{\pi \sqrt{1 - \lambda(\epsilon + 1)}}{2K \left(\frac{2\epsilon\lambda}{(\epsilon + 1)\lambda - 1} \right)} \sqrt{2\mathcal{E}}, \quad \int_0^{1/(1+\epsilon)} d\lambda \overline{\left(\frac{v_{\parallel}}{B} \right)} = \frac{2}{3} \sqrt{2\mathcal{E}} (1 - 1.6\epsilon^{3/2} + O(\epsilon^2)), \tag{3.9a,b}$$

where, K is the complete elliptic integral of the first kind and $\lambda = \mu B_0/\mathcal{E}$ is the pitch angle variable (Helander & Sigmar 2005) with a range of $(0, 1/(1 + \epsilon))$. The lower limit corresponds to CPs with $\mu = 0$ and the upper limit corresponds to barely circulating particles on the separatrix with $\mathcal{E} = \mu B_{\max} = \mu B_0(1 + \epsilon)$. In terms of λ , we have $v_{\parallel} d^3 v = 2\pi(B/B_0)\mathcal{E} d\lambda d\mathcal{E}$. Assuming F_0 to be a Maxwellian and performing the energy integral \mathcal{E} from $(0, \infty)$, we obtain

$$\tilde{U}_{\parallel 1} = -(2\epsilon \cos \theta + 1.6\epsilon^{3/2} + O(\epsilon^2)) \frac{I\tilde{\varphi}'}{B}, \tag{3.10}$$

where $I\varphi'/B$ can be seen to be of $O(qU_E/\epsilon)$, which is the precession drift. We note that the parallel flow, (3.10), is smaller than the toroidal precession speed expected of

the TPs, by a factor of ϵ . In particular, given the large precession, we find a much larger angular momentum contribution from the TPs (even given the lower density fraction of this species). To examine this further, we calculate separately for trapped and circulating species the parallel flows resulting from the RH solution. Using (3.8) and integrating only over $\mathcal{E} > \mu B_{\max}$, we get for circulating particles (CP)

$$(n\tilde{U}_{\parallel})^{\text{CP}} = n_0(-2\epsilon \cos \theta + (-1.6 + (1 + \cos \theta)^{3/2})\epsilon^{3/2} + O(\epsilon^2))\frac{I\tilde{\varphi}'}{B}, \quad (3.11)$$

where we have used an expansion in ϵ . This flow speed is $O(qU_E)$ as expected. Correspondingly, for the trapped particles (TP), we integrate inside the separatrix over $\mu B_{\min} < \mathcal{E} < \mu B_{\max}$ to get for the parallel flow,

$$(n\tilde{U}_{\parallel})^{\text{TP}} = n_0(-(1 + \cos \theta)^{3/2}\epsilon^{3/2} + O(\epsilon^{5/2}))\frac{I\tilde{\varphi}'}{B}. \quad (3.12)$$

The total parallel flow is obtained by summing the last two expressions, giving

$$\tilde{U}_{\parallel} = -(2\epsilon \cos \theta + 1.6\epsilon^{3/2} + O(\epsilon^2))\frac{I\tilde{\varphi}'}{B}, \quad (3.13)$$

in agreement with (3.10). Note that, we expect to see a large toroidal precession from the TPs. Instead, we find from (3.12), the flow of the TP to be $O(qU_E)$ since the density of TP is $O(\sqrt{\epsilon})$. This is smaller than the toroidal precession drift of the TPs by a factor of ϵ . Further, if we calculate the poloidal velocity of the trapped particle fraction, we find

$$\mathbf{U}^{\text{TP}} \cdot \hat{\theta} = (u_{\parallel}^{\text{TP}} + U_E) \cdot \hat{\theta} \approx U_E; \quad (3.14)$$

the trapped particles seem to have a non-zero bounce averaged poloidal flow. This is puzzling, since for adiabatic changes we expect TPs to have a purely toroidal flow.

3.2. Angular momentum conservation and the effective mass

Inserting the parallel flow (3.10) into (2.4), we get the angular momentum equation in the form

$$\left(1 + 2q^2 + 1.6\frac{q^2}{\sqrt{\epsilon}} + O(q^2)\right) \partial_t \tilde{\varphi} = \tau_{\perp}. \quad (3.15)$$

From (3.15) we see that the factor multiplying $\partial_t \tilde{\varphi}$ is the Rosenbluth–Hinton coefficient. As clarification, we note that we have calculated the RH coefficient using the angular momentum equation. An equivalent way of doing this would be to use quasineutrality of the charged species. In the former approach, which is also a statement of quasineutrality in axisymmetry, only linear terms in v_{\parallel} are needed. In the latter approach, the calculation would have to be carried to a quadratic level (Xiao *et al.* 2007).

Equation (3.15) is of the form of Newton's law $\tau_{\perp} = Ma$ where the acceleration is the rate of change of U_E and M is the effective mass. Thus, we can say the RH coefficient plays the role of an effective mass. The $(1 + 2q^2)$ coefficient is the well-known Pfirsch–Schlüter coefficient (Hassam & Kulsrud 1978; Hirshman 1978) arising from the circulating particles response. We see that $1.6q^2/\sqrt{\epsilon}$ is the dominant term.

Using $\int_0^{2\pi} d\theta / (2\pi) (1 + \cos \theta)^{3/2} \approx 1.2$, it can be checked from (3.11), (3.12) that the averaged TP and CP flows are approximately in the ratio 1.2 : 0.4. The effective mass contributions are, respectively, $1.2q^2/\sqrt{\epsilon}$ due to the TPs and $0.4q^2/\sqrt{\epsilon}$ due to the CPs.

Given that we are doing a perturbative analysis, one might certainly question the validity of trapped particles staying trapped. However, we could consider very deeply trapped particles which cannot be detrapped easily. Moreover, it must be realized that we can make the dynamics arbitrarily slow by appropriately weakening τ_{\perp} and thus approach a quasi-static equilibrium. In such a situation we do expect to have well confined trapped particles. In each case, the above analysis would point out to discrepancies in trapped particle flows and contribution to the effective mass.

In order to understand the discrepancy between the RH solution and the expected TP contribution to the flows and, possibly, effective mass, we will now take a different approach to solve the low frequency RH problem.

4. Shifted coordinates

As shown earlier, in axisymmetry we can rewrite the DKE as

$$\frac{\partial f}{\partial t} + \left(v_{\parallel} + \frac{I\varphi'}{B} \right) \nabla_{\parallel} v_{\parallel} f + \left(v_{\parallel} \frac{I\varphi'}{B} - \mu B \right) \frac{\nabla_{\parallel} B}{B} \frac{\partial f}{\partial v_{\parallel}} = 0. \tag{4.1}$$

where $f = f(v_{\parallel}, \mu, \mathbf{x}, t)$. We reiterate that this equation is valid for large q and with U_E ordered to be of the same order as v_{th}/q . It can be deduced from this equation, by examining the characteristics, that $\mathcal{E}_* = (1/2)v_{\parallel}^2 + \mu B + I\varphi'(v_{\parallel}/B)$ is a constant of motion, as can be checked by a direct substitution into (4.1). Physically, the difference $I\varphi'v_{\parallel}/B$ between \mathcal{E}_* and \mathcal{E} is due to the electrostatic potential difference experienced by a particle undergoing a banana orbit. We have shown this in appendix A and it is also discussed elsewhere (Hassam 1996; Kagan & Catto 2008; Landreman & Catto 2010). Thus, any distribution function $f(\mathcal{E}_*)$ defines an equilibrium for kinetic MHD in an axisymmetric tokamak. Hence we shift to $(\mathcal{E}_*, v_{\parallel*})$ coordinates, defined as follows:

$$\left. \begin{aligned} \mathcal{E}_* &= \frac{1}{2}v_{\parallel}^2 + \mu B + I\varphi' \frac{v_{\parallel}}{B} = \mathcal{E} + \frac{I\varphi'v_{\parallel}}{B}, \\ v_{\parallel*} &= v_{\parallel} + \frac{I\varphi'}{B}, \quad d^3v = \sum_{\sigma} \frac{B d\mu d\mathcal{E}_*}{|v_{\parallel*}|} \end{aligned} \right\} \tag{4.2}$$

Here, $\sigma = \text{sign } v_{\parallel*}$ denotes the three regions in energy space, namely, the trapped population and the rightward and leftward moving circulating particle populations. The coordinate $v_{\parallel*}$ is defined with respect to coordinates shifted downward in v_{\parallel} . \mathcal{E}_* is then a downshifted energy-like coordinate, centred about $v_{\parallel*} = 0$. This shift, of size $\Delta = I\varphi'/B \approx qU_E/\epsilon$ in v_{\parallel} , is depicted in figure 3. In \mathcal{E}_* coordinates, centred with respect to $v_{\parallel*}$, the DKE, equation (2.5) or (4.1), becomes

$$\frac{\partial f}{\partial t} + v_{\parallel*} \nabla_{\parallel} |_{\mathcal{E}_*} f + \frac{\partial I\varphi'}{\partial t} \frac{v_{\parallel}}{B} \frac{\partial f}{\partial \mathcal{E}_*} = 0, \tag{4.3}$$

where $f = f(\mathcal{E}_*, \mu, \psi, \theta, t)$ and $\partial/\partial t$ is at constant \mathcal{E}_* . The angular momentum equation, also recast in \mathcal{E}_* coordinates, is now given by

$$\partial_t \left\langle n_0 \varphi' \frac{|\nabla \psi|^2}{B^2} \right\rangle - \partial_t \left\langle \int \sum_{\sigma} \frac{B d\mu d\mathcal{E}_*}{|v_{\parallel*}|} \frac{Iv_{\parallel} f}{B} \right\rangle = \tau_{\perp}. \tag{4.4}$$

In what follows, we shall use equations (4.2), (4.3), (4.4).

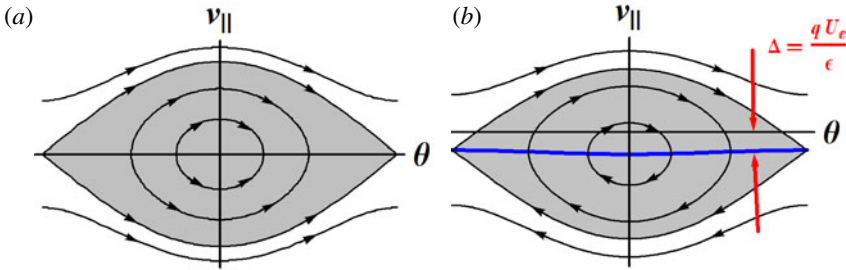


FIGURE 3. Contours of constant \mathcal{E} (a) and \mathcal{E}_* (b). The downward shift is given by the precession drift ($= I\varphi'/B \sim qU_E/\epsilon$).

5. The sub-bounce problem revisited

To make contact with the RH problem, we begin by performing a $\partial_t \ll \omega_b$ expansion, but allowing a large $U_E \sim v_{th}/q$, which corresponds to a finite downward shift as shown in figure 3. This approach allows for a more transparent calculation. To dominant order, we have from (4.3)

$$v_{\parallel*} \nabla_{\parallel} |_{\mathcal{E}_*} f \approx 0 \Rightarrow f = f(\mathcal{E}_*, t). \tag{5.1}$$

Annihilating the $\nabla_{\parallel \mathcal{E}_*}$ operator by bounce averaging gives a constraint equation for $f(\mathcal{E}_*, t)$, viz.

$$\frac{\partial f}{\partial t} + \frac{\partial I\varphi'}{\partial t} \overline{\left(\frac{v_{\parallel}}{B}\right)} \frac{\partial f}{\partial \mathcal{E}_*} = 0. \tag{5.2}$$

The constraint on f introduces a σ dependence. Equation (5.2) and the angular momentum relation (4.4), with $f = f(\mathcal{E}_*, t)$, form a closed set for the nonlinear $\{f, \varphi'\}$ system. We now do a subsidiary expansion in small $(I\varphi'/B) \ll v_{th}$, denoting $f = f_0 + f_1 + \dots$ (here, the subscript indices are not the same expansion parameter as in earlier sections). From (5.2), the corresponding lowest- and first-order equations are

$$\left. \frac{\partial f_0}{\partial t} \right|_{\mathcal{E}_*} = 0 \Rightarrow f_0 = f_0(\mathcal{E}_*), \tag{5.3a}$$

$$\frac{\partial f_1}{\partial t} + \frac{\partial I\varphi'}{\partial t} \overline{\left(\frac{v_{\parallel}}{B}\right)} \frac{\partial f_0}{\partial \mathcal{E}_*} = 0 \Rightarrow f_1 = -I\varphi' \overline{\left(\frac{v_{\parallel*}}{B}\right)} \frac{\partial f_0}{\partial \mathcal{E}_*}, \tag{5.3b}$$

where the overbar corresponds to the bounce average holding \mathcal{E}_*, μ constant, and we note that $\overline{(v_{\parallel*}/B)} = 0$ for TPs.

5.1. RH flows

We can now calculate the RH flows from (5.3). For general $(I\varphi'/B)/v_{th}$, the dominant-order parallel flow for either the TP or the CP populations (or both) is

$$(nU)_{\parallel} = \int \sum_{\sigma} \frac{B d\mu d\mathcal{E}_*}{|v_{\parallel*}|} v_{\parallel} f = \int \sum_{\sigma} \frac{B d\mu d\mathcal{E}_*}{|v_{\parallel*}|} \left(\sigma |v_{\parallel*}| - \frac{I\varphi'}{B} \right) f, \tag{5.4}$$

where, the integrals are to be taken over the appropriate populations and we have used the definition of $v_{\parallel*}$ as in (4.2). If we were to expand in small φ' , correct to first order, we would insert both $f = f_0 + f_1$ in the right-hand side integral in (5.4). However, since f_0 is independent of σ for both species, the lowest-order term, proportional to $\sigma |v_{\parallel*}| f_0$, will vanish, by symmetry (with respect to the \mathcal{E}_* coordinates). To first order then, two terms must be retained: one from the φ' term in the parenthesis and the other from the f_1 term. This yields the expression

$$(nU)_{\parallel} = \int \sum_{\sigma} \frac{B d\mu d\mathcal{E}_*}{|v_{\parallel*}|} \left(v_{\parallel*} f_1 - \frac{I\varphi'}{B} f_0 \right). \tag{5.5}$$

We emphasize that the second term in the integrand appears because of a ‘shift in the Jacobian’, and acts on the lowest order f . In particular, note that even for small φ' , this term must be retained as it is of the same order as the preceding f_1 term. Inserting for f_1 in (5.5), we have

$$(nU)_{\parallel} = -I\varphi' \int \sum_{\sigma} B d\mu d\mathcal{E}_* \left(\overline{\left(\frac{v_{\parallel*}}{B} \right)} \frac{\partial f_0}{\partial \mathcal{E}_*} + \frac{1}{|v_{\parallel*}| B} f_0 \right), \tag{5.6}$$

where, for TPs, we recall that $\overline{(v_{\parallel*}/B)} = 0$. (Equation (5.6) can be compared with (3.8), the corresponding equation from the previous section; the latter equation does not have a Jacobian shift term.)

Since $\overline{(v_{\parallel*}/B)} = 0$ for TPs, the TP parallel flow from (5.6) is

$$(nU)_{\parallel}^{\text{TP}} = -\frac{I\varphi'}{B} \int_{\text{TP}} \sum_{\sigma} \frac{B d\mu d\mathcal{E}_*}{|v_{\parallel*}|} f_0^{\text{TP}}(\mathcal{E}_*, t) = -n^{\text{TP}} \frac{I\varphi'}{B}, \tag{5.7}$$

where

$$n^{\text{TP}} = n_0 \left(\sqrt{\epsilon(1 + \cos \theta)} + \frac{\epsilon^{3/2}(\cos \theta + \cos 2\theta)}{2\sqrt{\cos \theta + 1}} + O(\epsilon^2) \right), \tag{5.8}$$

is the trapped particle density. This parallel flow is a rigid rotor flow and, we note, has an amplitude that corresponds precisely to the precession drift speed. We can also calculate the net poloidal velocity of the TPs,

$$\mathbf{U}^{\text{TP}} \cdot \hat{\theta} = \int d^3v f_0^{\text{TP}}(\mathbf{b}v_{\parallel} + \mathbf{U}_E) \cdot \hat{\theta}, \tag{5.9}$$

using (5.7), and we find

$$(n\mathbf{U})^{\text{TP}} \cdot \hat{\theta} = \frac{\epsilon}{q} \left((nU)_{\parallel}^{\text{TP}} + \frac{I\varphi'}{B} n^{\text{TP}} \right) = 0. \tag{5.10}$$

This is zero as expected. Thus, as we can see, the previously discussed discrepancies in TP parallel flow and TP theta flow have been resolved; we note that the ‘Jacobian shift’ is responsible for resolving the discrepancies. Importance of an analogous shift in a time dependent problem has been recently shown by Burby (2016).

The CP flow can now be calculated from (5.6) assuming that the lowest-order distribution function is a Maxwellian. This gives us

$$(nU)_{\parallel}^{\text{CP}} = n_0 \frac{I\varphi'}{B_0} \left(\sqrt{\epsilon(1 + \cos \theta)} - 2\epsilon \cos \theta + \epsilon^{3/2} \left(-1.6 + \frac{(\cos \theta + \cos 2\theta)}{2\sqrt{\cos \theta + 1}} \right) + O(\epsilon^2) \right). \tag{5.11}$$

Note that, to lowest order, the CP flow is a rigid rotor flow, equal and opposite to the TP flow. Thus from equations (5.11), (5.7) we see that to dominant order, $(nU_{\parallel})^{\text{CP}} + (nU_{\parallel})^{\text{TP}} \approx 0$. This says that in the accounting of parallel flows for angular momentum, the large TP precession flow does not materialize as a large parallel flow since it is completely balanced by an oppositely directed CP flow. The $\cos \theta$ term in the CP flow is the usual harmonic parallel flow. The net poloidal velocity of the CPs is:

$$\mathbf{U}^{\text{CP}} \cdot \hat{\theta} = \int d^3 f_0^{\text{CP}} v(\mathbf{b}v_{\parallel} + \mathbf{U}_E) \cdot \hat{\theta} = \frac{\epsilon}{q} \left(\frac{I\varphi'}{B_0} n^{\text{CP}} + O(\sqrt{\epsilon}) \right) \approx \mathbf{U}_E \cdot \hat{\theta}. \tag{5.12}$$

Hence the poloidal velocity of the CPs is basically the $\mathbf{E} \times \mathbf{B}$ flow, consistent with expectations.

Summing over the TP and CP flows, we get the total RH flow to be

$$(nU_{\parallel})^{\text{TP+CP}} = -\frac{I\varphi'}{B_0} (2\epsilon \cos \theta + 1.6\epsilon^{3/2} + O(\epsilon^2))n_0. \tag{5.13}$$

Although the individual flows, equations (5.7), (5.11), differ from the ones obtained using standard neoclassical methods, equations (3.12), (3.11), the total flows, equations (5.13), (3.13) from our calculation, match the RH solution. Remarkably, the large TP precession flow is balanced by an equally large and oppositely directed flow from the barely CPs.

5.2. RH Effective mass

We now consider the effective mass coefficient. For this, we would insert $f_0 + f_1$ just found into the second term of the angular momentum equation (4.4). The second term

$$\partial_t \left\langle \int \sum_{\sigma} \frac{B d\mu d\mathcal{E}_*}{|v_{\parallel*}|} \frac{Iv_{\parallel}}{B} f \right\rangle \tag{5.14}$$

is just the time derivative of the parallel flow, viz., $\partial_t \langle (I/B)(nU_{\parallel}^{\text{total}}) \rangle$. A general expression for the parallel flow (for small φ') is given by (5.6). Inserting this expression as discussed, we obtain the angular momentum equation as

$$\partial_t \left\langle \varphi' \frac{|\nabla \psi|^2}{B^2} \right\rangle + \partial_t \left\langle I^2 \varphi' \left(\frac{1}{B^2} + \int_{\text{CP}} \sum_{\sigma} \frac{B d\mu d\mathcal{E}_*}{|v_{\parallel*}|n_0} \frac{v_{\parallel*}}{B} \overline{\left(\frac{v_{\parallel*}}{B} \right)} \frac{\partial f_0}{\partial \mathcal{E}_*} \right) \right\rangle = \tau_{\perp}. \tag{5.15}$$

Rearranging, we find

$$\partial_t \mathbf{U}_E = \frac{F_{\perp}/m}{1 + \mathcal{D}}, \tag{5.16}$$

where,

$$\begin{aligned} \mathcal{D} &= \left\langle \left(\frac{1}{B^2} + \int_{\text{CP}} \sum_{\sigma} \frac{B d\mu d\mathcal{E}_*}{|v_{\parallel*}|n_0} \frac{v_{\parallel*}}{B} \overline{\left(\frac{v_{\parallel*}}{B} \right)} \frac{\partial f_0}{\partial \mathcal{E}_*} \right) \right\rangle \left\langle \frac{|\nabla \psi|^2}{I^2 B^2} \right\rangle^{-1} \\ &\approx \frac{q^2}{\epsilon^2} \langle nU_{\parallel}^{\text{total}} \rangle / (I\varphi'/B_0), \end{aligned} \tag{5.17}$$

represents the added effective mass.

To illuminate the role of each species in the effective mass, we consider the individual effective mass contributions from the TPs and CPs. Using $\int_0^{2\pi} d\theta (\cos \theta + \cos 2\theta) / (4\pi\sqrt{\cos \theta + 1}) \approx 0.15$, the TP contribution to the effective mass coefficient can be shown to be

$$\frac{q^2}{\epsilon^2} \langle nU_{\parallel}^{\text{TP}} \rangle / (I\phi' / B_0) \sim \frac{q^2}{\epsilon^{3/2}} + 0.15 \frac{q^2}{\sqrt{\epsilon}} + O(q^2). \tag{5.18}$$

Thus the effective mass contribution from the TPs is $\sim O(q^2/\epsilon^{3/2}) \gg 1$ as expected from our toy model. The CP contribution to the effective mass coefficient is

$$\frac{q^2}{\epsilon^2} \langle nU_{\parallel}^{\text{CP}} \rangle / (I\phi' / B_0) \sim -\frac{q^2}{\epsilon^{3/2}} + 1.45 \frac{q^2}{\sqrt{\epsilon}} + O(q^2). \tag{5.19}$$

To lowest order this is equal and opposite to the TP effective mass. Thus the total effective mass is $1 + 1.6q^2/\sqrt{\epsilon} + O(q^2)$, consistent with the original RH calculation.

5.3. Flows and effective masses for truncated distributions

We have seen that the cancellation of the rapid TP precession flow by an oppositely directed flow of barely CPs explains why the effective mass is smaller than that expected from the TPs alone. But this finding does not unequivocally address whether a distribution function of only TPs would result in the expected large effective mass. To address this, we consider the distribution function in (5.17) to be populated only for $\mathcal{E}_* < \mu B_{\text{max}}$. For this case, the TP contribution to the effective mass can be seen from (5.18) to be independent of the details of the distribution. The contribution is found to be $\sim (q^2/\epsilon^2)n^{\text{TP}}$. Since there are no CPs, $n^{\text{TP}} = n$. Therefore, we find the effective mass to be q^2/ϵ^2 , and the accompanying TP flows to be

$$U_{\parallel}^{\text{TP}} = -\frac{I\phi'}{B}, \quad \mathbf{U}^{\text{TP}} \cdot \hat{\theta} = 0. \tag{5.20a,b}$$

To complete this line of reasoning, we have considered a distribution function with only energetic CPs, i.e. all particles considered to lie well above the separatrix region ($\mathcal{E}_* = \mu B_0(1 + \epsilon)$) in phase space. The effective mass can be shown to be $1 + O(q^2)$. These results are consistent with fluid models where we get the oscillating Pfirsch–Schluter flows and the corresponding effective mass coefficient. We also find that unless we approach the separatrix, there are no $\sqrt{\epsilon}$ terms.

The above findings for TP and CP flows are fully consistent with our toy model equation (1.2) which shows the $O(q^2/\epsilon^2)$ effective mass contribution from the trapped particle and the $O(1)$ contribution from the freely circulating particle.

6. The role of the barely circulating particles

We have shown that the large trapped particle precession flow is cancelled to lowest order by an opposite flow from the circulating particles, so that there are no large composite flows of order $qU_E/\sqrt{\epsilon}$. We would now like to understand the origin of the opposite flow. We show here that this flow is largely from a class of barely circulating particles. To demonstrate this, we begin with a more sophisticated toy model. Consider a particle on a rod as shown in figure 4. The generalized coordinates

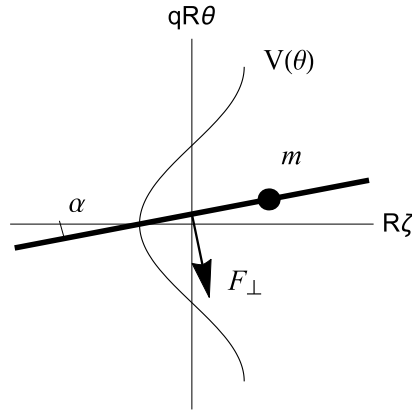


FIGURE 4. Upgraded bead-on-wire toy model showing a particle of mass m moving along a field line inclined at an angle $\alpha \approx \epsilon/q$ to the toroidal direction. The field line moves rigidly under applied force F_{\perp} . The particle also feels the mirror force, modelled by the potential $V(\theta)$, as it moves along \mathbf{B} .

are $(x = R_0\zeta, y = qR_0\theta)$, where θ, ζ are analogous to the poloidal and toroidal angles. In addition to being constrained to move only along the rod, the particle also feels a force due to an applied potential $V(\theta) = \mu B(\theta) = \mu B_0(1 - \epsilon \cos \theta)$. Here, the force from the potential, $V(\theta)$, corresponds to the $\mu \nabla_{\parallel} B$ force, the mirror force that the particle feels as it moves in θ along \mathbf{B} . Thus, while our previous model allowed only freely circulating particles and deeply trapped particles, our new model allows these but also allows barely circulating particles.

The Lagrangian is given by,

$$L(\theta, \dot{\theta}, \zeta, \dot{\zeta}) = \frac{1}{2}mR_0^2((q\dot{\theta})^2 + (\dot{\zeta} + q\dot{\theta} \cot \alpha)^2) - \mu m B_0(1 - \epsilon \cos \theta) - mR_0^2 c(t) \dot{\zeta}, \quad (6.1)$$

where $c = (\int F_{\perp} dt) \sin \alpha / (mR_0)$ is the impulse due to the applied force F_{\perp} . Here we use the impulse instead of work done by the force in the Lagrangian to manifestly preserve axisymmetry.

The equation of motion is

$$\ddot{\theta} + \omega_b^2 \sin \theta = -\frac{F_{\perp} \cos \alpha}{qmR_0} \quad \text{where } \omega_b = \sqrt{\mu B_0 \epsilon} / qR_0, \quad (6.2)$$

which shows that our toy model is identical to a driven nonlinear pendulum (Henrard 2005). We can exploit this similarity to understand the particle trajectories in the presence of the external torque. Let us consider the case where F_{\perp} is time independent. In this case the work and energy \mathcal{E} of the driven pendulum is conserved. Thus,

$$\mathcal{E} = \frac{1}{2}\dot{\theta}^2 - \omega_b^2 \cos \theta + \frac{F_{\perp} \cos \alpha}{qmR_0} \theta = \text{const.} \quad (6.3)$$

Figure 5 shows the contours of constant \mathcal{E} for non-zero F_{\perp} . Note that for small F_{\perp} , most of the trajectories resemble the original trajectories of a torque-free pendulum. However now there exists a group of barely circulating particles near the separatrix (shown in red in figure 5), which can change directions so that the final direction is in the same sense as the applied torque.

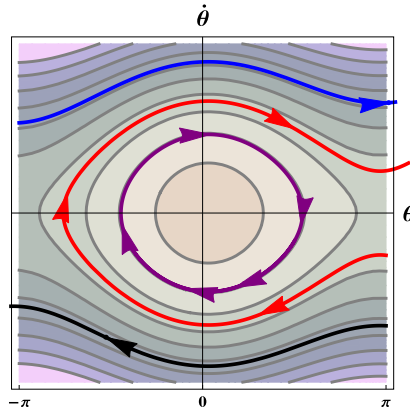


FIGURE 5. Phase portrait of a pendulum driven by F_{\perp} . In black and blue we show oppositely moving freely circulating particle. In purple we show the orbit of a deeply trapped particle and in red we show a barely circulating particle preferentially changing direction in the presence of small F_{\perp} .

In order to make contact with the drift-kinetic system, let's now use the Hamiltonian description of the toy model. From the Lagrangian we calculate the canonical momenta,

$$\frac{P_{\theta}}{mR_0^2} = \dot{\zeta} \cot \alpha + q\dot{\theta}/\sin^2 \alpha, \quad \frac{P_{\zeta}}{mR_0^2} = \dot{\zeta} - c + q\dot{\theta} \cot \alpha. \tag{6.4a,b}$$

Since the Lagrangian is independent of ζ , the ‘toroidal angle’, P_{ζ} must be a constant. The Hamiltonian \mathcal{H} , can now be constructed,

$$\mathcal{H}/m - \frac{1}{2} \left(\frac{P_{\zeta}}{mR_0} + R_0c \right)^2 = \frac{1}{2} v_{\parallel*}^2 + \mu B(\theta), \tag{6.5}$$

where, $v_{\parallel*} \equiv qR_0\dot{\theta} = (P_{\theta} - q \cot \alpha (P_{\zeta} + cmR_0^2))/qm$. We can now define $\mathcal{E}_* = (1/2)v_{\parallel*}^2 + \mu B(\theta)$ and write down Liouville’s equation for this system in $\{\theta, \zeta, \mathcal{E}_*, P_{\zeta}\}$ coordinates. We restrict ourselves to the ‘axisymmetric’ problem by choosing $\partial_{\zeta} = 0$ (in axisymmetry there always exists a local frame). Thus we have,

$$\frac{\partial f}{\partial t} + \frac{v_{\parallel*}}{qR_0} \frac{\partial f}{\partial \theta} - \frac{\partial}{\partial t} (R_0c \cot \alpha) v_{\parallel*} \frac{\partial f}{\partial \mathcal{E}_*} = 0. \tag{6.6}$$

Let us compare the Liouville’s equation (6.6) with the drift-kinetic equation (4.3). We note that, by making the identification $I\phi'/B \iff -R_0c \cot \alpha$, we obtain a one–one relation. This is perhaps not surprising because both equations describe conservation of phase space volume.

Let us now try to understand the large cancellation of the RH flows. From the DKE–toy model equivalence, we see that $I\phi'/B \propto -F_{\perp}$. Figure 5 now corresponds to the case where $I\phi'/B > 0$. We have already seen that the trapped particles precess with speed $u_{\parallel}^{\text{TP}} \approx qU_E/\epsilon$. Their net flow from equation (5.7) is $(nu_{\parallel})^{\text{TP}} = -n\sqrt{\epsilon}I\phi'/B$ which is negative in this case. The barely circulating particles on the other hand, have a similar density, $\sqrt{\epsilon}$, but have an opposite flow $n\sqrt{\epsilon}I\phi'/B > 0$ (see (5.11)). Thus the two flows cancel. A further explanation of the opposite flows is provided in the next section and in appendix D.

7. Sub-bounce dynamics in collisionless axisymmetric systems with sub-poloidal sonic flows

The analysis presented in § 5 was restricted to small flows. In this section, we present a nonlinear generalization of this analysis to finite but sub-poloidal sonic flows. We shall relax these constraints further in appendix D. Our main result in this section is to show that the collisionless RH flows and effective inertia arise because of two physical principles: conservation of angular momentum owing to axisymmetry, and conservation of J_{\parallel} due to sub-bounce nature of the flows.

We shall first show that the distribution function f_0 is a function of the second adiabatic invariant $J_{\parallel} = \oint v_{\parallel} dl$ by solving (5.2) exactly. This is perhaps not surprising, since in the drift ordered sub-bounce kinetic system, J_{\parallel} is conserved (Medvedev *et al.* 1998), provided the forcing is adiabatic. Here we shall be content in restricting ourselves to sub-bounce axisymmetric systems. The existence of a second adiabatic invariant for kinetic MHD in more general settings has been discussed recently (Burby & Sengupta 2017). The second adiabatic invariant J_{\parallel} is defined by

$$J_{\parallel} = \oint_{\mathcal{E}_*} v_{\parallel} dl = \oint_{\mathcal{E}_*} v_{\parallel*} dl - \sigma q R \frac{I\varphi'}{B_0}. \tag{7.1}$$

We note that the J_{\parallel} integral is done along a field line holding \mathcal{E}_* fixed. Using $\mathcal{E}_* = v_{\parallel}^2/2 + \mu B + v_{\parallel} I\varphi'/B$ and $v_{\parallel*} = v_{\parallel} + I\varphi'/B$, we can show that

$$\frac{\partial v_{\parallel}}{\partial \mathcal{E}_*} = \frac{1}{v_{\parallel*}}, \quad \frac{\partial v_{\parallel}}{\partial t} \Big|_{\mathcal{E}_*} = -\frac{1}{v_{\parallel*}} \frac{v_{\parallel}}{B} \partial_t I\varphi', \tag{7.2a,b}$$

$$\frac{\partial J_{\parallel}}{\partial \mathcal{E}_*} = \oint_{\mathcal{E}_*} \frac{dl}{v_{\parallel*}}, \quad \partial_t J_{\parallel} = -\oint_{\mathcal{E}_*} \frac{dl}{v_{\parallel*}} \frac{v_{\parallel}}{B} \partial_t I\varphi', \tag{7.2c,d}$$

where the time derivative is done at fixed $(\mu, \mathcal{E}_*, \psi, \theta)$ and \mathcal{E}_* derivative is at constant (μ, θ, ψ, t) . We can now simplify (5.2) using the above properties of J_{\parallel} .

$$\frac{\partial f_0}{\partial t} + \frac{\partial I\varphi'}{\partial t} \left(\frac{v_{\parallel}}{B} \right) \frac{\partial f_0}{\partial \mathcal{E}_*} = 0 \quad \Rightarrow \quad \frac{\partial f_0}{\partial t} \frac{\partial J_{\parallel}}{\partial \mathcal{E}_*} - \frac{\partial J_{\parallel}}{\partial t} \frac{\partial f_0}{\partial \mathcal{E}_*} = 0. \tag{7.3}$$

The last equation clearly implies $f_0 = f_0(J_{\parallel})$. Such a solution has been previously obtained by Kulsrud (1961) treating U_E as a perturbation. Our result allows large flows.

Note the crucial sigma dependence in the expression for J_{\parallel} as noted earlier (Hastie, Taylor & Haas 1967; Henrard 2005). There is no such sigma dependence in the trapped particle distribution because the second term averages out as $\sigma = \pm 1$ for TPs. This means that the CP distribution is not symmetric with respect to $v_{\parallel*} = 0$.

In MHD ordering, the net flow is given by $\mathbf{U} = (U_{\parallel}/B)\mathbf{B} + \mathbf{U}_E$ with $\mathbf{U}_E = \mathbf{B} \times \nabla\varphi(\psi)/B^2$. In an axisymmetric system, using (2.3), we get the following expression for the net flow

$$\mathbf{U} = F\mathbf{B} - \varphi'R^2\nabla\zeta, \quad F \equiv \frac{1}{B} \left(U_{\parallel} + \frac{I\varphi'}{B} \right). \tag{7.4a,b}$$

From the definition of U_{\parallel} we obtain,

$$n_0 F = \int d^3v \frac{v_{\parallel*}}{B} f_0 = \sum_{\sigma_*} \int d\mu d\mathcal{E}_* f_0(\mathcal{E}_*). \tag{7.5}$$

Let us now consider the angular momentum conservation equation

$$\partial_t \langle n_0 \mathbf{U} \cdot \mathbf{R}^2 \nabla \zeta \rangle = -\tau_{\perp}, \tag{7.6}$$

where τ_{\perp} is defined as in (2.4). Substituting for \mathbf{U} from (7.4) into (7.6) we get

$$\langle n_0 R^2 \rangle \partial_t \varphi' - I \partial_t \langle n_0 F \rangle = \tau_{\perp}. \tag{7.7}$$

In order to evaluate (7.7) we need an evolution equation for $n_0 F$. From (7.5) we get

$$\partial_t (n_0 F) = \sum_{\sigma_*} \int d\mu d\mathcal{E}_* (\partial_t J_{\parallel}) \frac{\partial f_0}{\partial J_{\parallel}} = -\partial_t \varphi' \sum_{\sigma_*} \int \frac{d\mu d\mathcal{E}_*}{|v_{\parallel*}| n_0} v_{\parallel*} \left(\frac{v_{\parallel}}{B} \right) \frac{\partial f_0}{\partial \mathcal{E}_*}. \tag{7.8}$$

For the flows to be divergence free we need $\nabla \cdot (n\mathbf{U}) = 0$ which implies $\mathbf{B} \cdot \nabla (nF) = 0$ from (7.4) due to axisymmetry. From (7.8) we see that the factor $v_{\parallel*}(\theta)$ cancels out and the right side is only a function of ψ after the \mathcal{E}_* and μ integrals are performed. Thus $\mathbf{B} \cdot \nabla (nF) = 0$ is satisfied and the flows are indeed divergence free as expected for a stationary state.

Using angular momentum conservation (7.7) and (7.8), we obtain the generalization of (5.17) for finite flow, showing a generalized effective mass,

$$\partial_t \varphi' \left(I^2 \left\langle \int d^3 v \left(\frac{v_{\parallel*}}{B} \right) \left(\frac{v_{\parallel}}{B} \right) \frac{\partial f_0}{\partial \mathcal{E}_*} \right\rangle + \langle n_0 R^2 \rangle \right) = \tau_{\perp}, \tag{7.9}$$

where f_0 can depend nonlinearly on φ . In the limit of small U_E/v_{th} , we recover (5.17) and hence the RH coefficient $(1 + 1.6q^2/\sqrt{\epsilon})$ in the large aspect ratio limit with an initial Maxwellian. The effective mass can also be written in terms of J_{\parallel} as shown in (D7).

Now let us try to understand the origin of the opposite flows from this point of view. Note that for small (U_E/v_{th}) , F is zero for TPs because the TP distribution function is an even function of $v_{\parallel*}$. This ensures that the poloidal flow of TPs is zero and the parallel flow is due to the fast precession. Also from (7.9), we can see that the TPs always contribute the large q^2/ϵ^2 effective mass. F is however non-zero and in fact different for the CPs above and below the separatrix. This breaks the up down symmetry dynamically, leading to differential parallel flow due to CPs. The fact that the CP flow must be opposite to the TPs also follow from the fact that J_{\parallel} must be conserved and that J_{\parallel} is initially small because of the initial up-down symmetry of the initial Maxwellian.

8. Summary

If a tokamak plasma is set into motion with an initial radial electric field E_r , the final state, after transients, is a much reduced E_r and a parallel zonal flow consistent with angular momentum conservation. However, the well-known trapped particle precession angular momentum in the final E_r field is much larger than the zonal flow. We have shown in this paper that this apparent paradox is resolved by the fact that there are reverse flows from the barely passing particles that cancel the large momentum from the TP precession momentum. Mathematically, we show that, even for small perturbations, there is a linear shift in the Jacobian of the phase space volume element, from E_r , that accounts for the reverse flows and the

cancellation. The effective mass for this system is the same as that obtained by Rosenbluth and Hinton (Rosenbluth & Hinton 1998) and Xiao *et al.* (2007). We have shown that sub-bounce axisymmetric kinetic MHD can be formulated in terms of the parallel adiabatic invariant J_{\parallel} much like the sub-bounce low flow drift-kinetic system. Rosenbluth–Hinton distribution function and the effective mass follows directly from J_{\parallel} conservation in the long wavelength limit. This is expected even in the long wavelength low flow drift ordered kinetic systems.

Acknowledgements

The authors would like to thank the anonymous referees for their thorough, constructive and helpful reviews. We also acknowledge stimulating discussion with R. M. Kulsrud, T. M. Antonsen Jr. W. Dorland, J. F. Drake and M. Landreman. W.S. would also like to acknowledge helpful advice from J. J. Ramos, I. Pusztai and P. J. Catto. This research was funded by the US DOE.

Appendix A. Relation of \mathcal{E}_* to toroidal angular momentum ψ_*

We shall now clarify the meaning of the shifted energy variable \mathcal{E}_* . It is well known (Kagan & Catto 2008) that in axisymmetry the conservation of canonical angular momentum leads to conservation of ψ_* defined as

$$\psi_* = \psi - \frac{M}{e} \mathbf{v} \cdot \mathbf{R}^2 \nabla \zeta \approx \psi - \frac{I v_{\parallel}}{\Omega} = \text{const.}, \quad \Omega = \frac{eB}{M}, \quad (\text{A } 1)$$

where \mathbf{v} is the velocity vector of particle of mass m and charge e . The contribution of perpendicular velocities to ψ_* average out except for U_E terms which are also negligible in our large sub-poloidal sonic ordering. The second term in ψ_* is smaller than the first by a factor of ρ_* ($\equiv \rho/L$) and is related to the finite banana width.

In a steady state collisionless plasma, total energy (kinetic plus electrostatic potential) is also conserved.

$$w = \frac{1}{2}(v_{\parallel}^2 + \mu B) + \frac{e}{M} \varphi(\psi) = \text{const.} \quad (\text{A } 2)$$

In drift ordering all the energy terms are one to one. However in MHD ordering, since $e\varphi/T = 1/\rho_*$ and $\rho_* \approx 0$, the conserved quantities must be evaluated order by order. To lowest order thus we have

$$\psi \approx \psi_* = \text{const.}, \quad w = \frac{e}{M} \varphi(\psi_*) = \text{const.} \quad (\text{A } 3a,b)$$

To next order,

$$\psi \approx \psi_* + \frac{I v_{\parallel}}{\Omega}, \quad (\text{A } 4)$$

$$\begin{aligned} \mathcal{E}_* &= \frac{1}{2}(v_{\parallel}^2 + \mu B) + \frac{e}{M} \varphi(\psi) - \frac{e}{M} \varphi(\psi_*) \\ &= \frac{1}{2}(v_{\parallel}^2 + \mu B) + \frac{I \varphi'}{B} = \text{const.}, \end{aligned} \quad (\text{A } 5)$$

where we have Taylor expanded $\varphi(\psi)$ about $\psi = \psi_* + O(\rho_*)$ to obtain \mathcal{E}_* . Thus, it is clear that \mathcal{E}_* is indeed a shifted total energy, the shift being the potential difference across a banana width. It is important to note that in kinetic MHD, ψ is needed only

to lowest order since the radial drifts are formally an order smaller than the parallel and the $\mathbf{E} \times \mathbf{B}$ drifts. Since $\psi = \psi_*$ to lowest order we are self-consistently ignoring $\dot{\psi}$ terms in the DKE. This does not interfere with energy conservation owing to \mathcal{E}_* . From the DKE it can be checked that for a time independent system, $\dot{\psi} = \dot{\mathcal{E}}_* = 0$, by direct substitution. Thus, equation (4.3) with the $\partial_t I \tilde{\varphi}'$ term is analogous to the standard drift ordered DKE (Hazeltine 1983) with the $(e/M)\partial_t \tilde{\varphi}$ term.

Appendix B. Vorticity equation in \mathcal{E} and \mathcal{E}_* coordinates

We can derive the vorticity equation using $\langle \mathbf{j} \cdot \nabla \psi \rangle = 0$. From Kulsrud’s equation (1980) (46), it can be shown that

$$\partial_t \left\langle n \frac{|\nabla \psi|^2}{B^2} \varphi' \right\rangle = \left\langle \int d^3 v \frac{e}{M} \mathbf{v}_d \cdot \nabla \psi f \right\rangle + \tau_\perp. \tag{B 1}$$

In an axisymmetric system,

$$\mathbf{B} \times \nabla \psi \cdot \nabla B = I \mathbf{B} \cdot \nabla B, \quad \nabla_{\parallel} |_{\mathcal{E}} \left(\frac{1}{2} v_{\parallel}^2 \right) = -\mu \nabla_{\parallel} B, \tag{B 2a,b}$$

and we can show that

$$\frac{e}{M} \mathbf{v}_d \cdot \nabla \psi = v_{\parallel} \nabla_{\parallel} |_{\mathcal{E}} \left(\frac{I v_{\parallel}}{B} \right) = -(v_{\parallel}^2 + \mu B) I \frac{\nabla_{\parallel} B}{B^2}. \tag{B 3}$$

Now,

$$\mathcal{E}_* = \frac{1}{2} v_{\parallel}^2 + \mu B + I \varphi' \frac{v_{\parallel}}{B} = \frac{1}{2} v_{\parallel*}^2 + \mu B - \left(\frac{I \varphi'}{B} \right)^2 \tag{B 4}$$

$$\Rightarrow \nabla_{\parallel} |_{\mathcal{E}_*} \left(\frac{1}{2} v_{\parallel*}^2 \right) = -\frac{\nabla_{\parallel} B}{B} \left(\mu B + \left(\frac{I \varphi'}{B} \right)^2 \right). \tag{B 5}$$

So,

$$v_{\parallel*} \nabla_{\parallel} |_{\mathcal{E}_*} \frac{v_{\parallel}}{B} = v_{\parallel*} \nabla_{\parallel} |_{\mathcal{E}_*} \left(\frac{v_{\parallel*}}{B} - \frac{I \varphi'}{B} \right) \tag{B 6}$$

$$= -(v_{\parallel}^2 + \mu B) \frac{\nabla_{\parallel} B}{B^2} = v_{\parallel} \nabla_{\parallel} |_{\mathcal{E}} \left(\frac{v_{\parallel}}{B} \right). \tag{B 7}$$

Appendix C. Proof of equivalence of angular momentum and vorticity equation

Using the following identities,

$$R^2 \nabla \zeta \cdot \mathbf{U}_E = -\frac{|\nabla \psi|^2}{B^2} \varphi', \quad R^2 \nabla \zeta \cdot \mathbf{b} = \frac{I}{B}, \tag{C 1a,b}$$

the angular momentum conservation condition (4.4), simplifies to

$$\begin{aligned} \partial_t \left\langle n \frac{|\nabla \psi|^2}{B^2} \varphi' \right\rangle - \tau_\perp &= \partial_t \left\langle \int d^3 v \frac{I v_{\parallel}}{B} f \right\rangle \\ &= \left\langle \int d^3 v \frac{I v_{\parallel}}{B} \left(\frac{\partial}{\partial t} \Big|_{\mathcal{E}_*} + \frac{\partial I \varphi'}{\partial t} \frac{v_{\parallel}}{B} \frac{\partial}{\partial \mathcal{E}_*} \right) f \right\rangle \\ &= \left\langle \int d^3 v \frac{I v_{\parallel}}{B} (-v_{\parallel*} \nabla_{\parallel} |_{\mathcal{E}_*} f) \right\rangle \\ &= \left\langle \int d^3 v \frac{e}{M} \mathbf{v}_d \cdot \nabla \psi f \right\rangle \quad (\text{integrating by parts}). \tag{C 2} \end{aligned}$$

Appendix D. J_{\parallel} invariance and the RH problem for arbitrary q and sub-poloidal sonic flows

So far we have presented a large q ordering. In this section we shall present the general result for arbitrary q . We shall still assume flows to be smaller than the poloidal sound speed in order to avoid Alfvénic resonances (Hassam 1996). The U_E^2 term previously neglected in the DKE (2.1), is now kept. The E_{\parallel} term is also kept to ensure quasineutrality, $n_e = n_i$, in the presence of large centrifugal forces. This motivates us to introduce $\varphi_1(\psi, \theta)$ such that $E_{\parallel} = -\nabla_{\parallel}\varphi_1$. U_E depends only on the lowest-order electrostatic potential, $\varphi = \varphi(\psi)$, which is still a flux function. We shall assume adiabatic electrons. In axisymmetry the ion DKE (2.1) can be written as

$$\frac{\partial f}{\partial t} + \left(v_{\parallel} + \frac{I\varphi'}{B} \right) \nabla_{\parallel}|_{v_{\parallel}} f + \left(\left(v_{\parallel} \frac{I\varphi'}{B} - \mu B \right) \frac{\nabla_{\parallel} B}{B} + \nabla_{\parallel} \left(\frac{U_E^2}{2} - \frac{e\varphi_1}{M} \right) \right) \frac{\partial f}{\partial v_{\parallel}} = 0, \tag{D 1}$$

where the last two terms come from $-\mathbf{b} \cdot \mathbf{U}_E \cdot \nabla \mathbf{U}_E$ and $(e/M)E_{\parallel}$. It is straightforward to show that for finite q , \mathcal{E}_* is given by

$$\mathcal{E}_* = \frac{1}{2}v_{\parallel}^2 + \frac{I\varphi'}{B}v_{\parallel} + \mu B + \frac{e\varphi_1}{M} - \frac{U_E^2}{2} = \frac{1}{2}v_{\parallel*}^2 + \mu B + \frac{e\varphi_1}{M} - \frac{1}{2}R^2\varphi'^2. \tag{D 2}$$

In \mathcal{E}_* coordinate we have

$$\frac{\partial f}{\partial t} + v_{\parallel*} \nabla_{\parallel}|_{\mathcal{E}_*} f + \dot{\mathcal{E}}_* \frac{\partial f}{\partial \mathcal{E}_*} = 0, \tag{D 3}$$

where $\dot{\mathcal{E}}_* = v_{\parallel*} \partial_t I\varphi'/B + \partial_t(e\varphi_1/m - R^2\varphi'^2/2)$ and $v_{\parallel*} = v_{\parallel} + I\varphi'/B$.

As before, we investigate the sub-bounce zonal flow problem by expanding $f = f_0 + f_1 + \dots$ and obtain the bounce averaged equation for f_0

$$\frac{\partial f_0}{\partial t} + \overline{\dot{\mathcal{E}}_*} \frac{\partial f_0}{\partial \mathcal{E}_*} = 0 \quad \Rightarrow \quad \left(\oint \frac{dl}{v_{\parallel*}} \right) \frac{\partial f_0}{\partial t} + \left(\oint \frac{dl}{v_{\parallel*}} \dot{\mathcal{E}}_* \right) \frac{\partial f_0}{\partial \mathcal{E}_*} = 0. \tag{D 4}$$

Once again using $J_{\parallel} = \oint_{\sigma_*} v_{\parallel} dl$ the above equation can be recast into

$$(\partial_{\mathcal{E}_*} J_{\parallel}) \partial_t f_0 - (\partial_t J_{\parallel}) \partial_{\mathcal{E}_*} f_0 = 0, \quad \Rightarrow \quad f_0 = f_0(J_{\parallel}). \tag{D 5}$$

Quasineutrality then gives us φ_1 in terms of φ' . The flow and angular momentum equations in this limit are completely identical to the equations (7.5), (7.4), (7.7) derived earlier and

$$\partial_t(n_0 F) = \sum_{\sigma_*} \int d\mu d\mathcal{E}_* \partial_t f_0 = \sum_{\sigma_*} \int d\mu d\mathcal{E}_* (\partial_t J_{\parallel}) \frac{\partial f_0}{\partial J_{\parallel}}. \tag{D 6}$$

Note that, since the only time dependence comes through φ' , $\partial_t J_{\parallel}$ is proportional to $\partial_t \varphi'$. The final evolution equation for φ' is now given by

$$\partial_t \varphi' \left(I \left\langle \sum_{\sigma_*} \int d\mu d\mathcal{E}_* \left(\frac{\partial J_{\parallel}}{\partial \varphi'} \right) \frac{\partial f_0}{\partial J_{\parallel}} \right\rangle + \langle n_0 R^2 \rangle \right) = \tau_{\perp}. \tag{D 7}$$

REFERENCES

- BURBY, J. W. 2016 The initial value problem in Lagrangian drift kinetic theory. *J. Plasma Phys.* **82** (3), doi:[10.1017/S0022377816000532](https://doi.org/10.1017/S0022377816000532).
- BURBY, J. W. & SENGUPTA, W. 2017 Hamiltonian structure of the guiding center plasma model, Preprint, [arXiv:1711.03992](https://arxiv.org/abs/1711.03992).
- BURRELL, K. H. 1997 Effects of $e \times b$ velocity shear and magnetic shear on turbulence and transport in magnetic confinement devices. *Phys. Plasmas* **4** (5), 1499–1518.
- CERFON, A. J. & FREIDBERG, J. P. 2011 Magnetohydrodynamic stability comparison theorems revisited. *Phys. Plasmas* **18** (1), 012505.
- DIAMOND, P. H., ITOH, S. I., ITOH, K. & HAHM, T. S. 2005 Zonal flows in plasma a review. *Plasma Phys. Control. Fusion* **47** (5), R35.
- DORLAND, W., JENKO, F., KOTSCHENREUTHER, M. & ROGERS, B. N. 2000 Electron temperature gradient turbulence. *Phys. Rev. Lett.* **85** (26), 5579.
- FRIEMAN, E., DAVIDSON, R. & LANGDON, B. 1966 Higher-order corrections to the Chew–Goldberger–low theory. *Phys. Fluids* **9** (8), 1475–1482.
- HASSAM, A. B. 1996 Poloidal rotation of tokamak plasmas at super poloidal sonic speeds. *Nucl. Fusion* **36** (6), 707.
- HASSAM, A. B. & KLEVA, R. G. 2011 Double adiabatic theory of collisionless geodesic acoustic modes in tokamaks, Preprint, [arXiv:1109.0057](https://arxiv.org/abs/1109.0057).
- HASSAM, A. B. & KULSRUD, R. M. 1978 Time evolution of mass flows in a collisional tokamak. *Phys. Fluids* **21** (12), 2271–2279.
- HASTIE, R. J., TAYLOR, J. B. & HAAS, F. A. 1967 Adiabatic invariants and the equilibrium of magnetically trapped particles. *Ann. Phys.* **41** (2), 302–338.
- HAZELTINE, R. D. 1983 Reduced magnetohydrodynamics and the Hasegawa–Mima equation. *Phys. Fluids* **26** (11), 3242.
- HELANDER, P. & SIGMAR, D. J. 2005 *Collisional Transport in Magnetized Plasmas*, vol. 4. Cambridge University Press.
- HENRARD, J. 2005 The adiabatic invariant theory and applications. In *Hamiltonian Dynamics. Theory and Applications*, pp. 77–141. Springer.
- HINTON, F. L. & WONG, S. K. 1985 Neoclassical ion transport in rotating axisymmetric plasmas. *Phys. Fluids* **28** (10), 3082–3098.
- HIRSHMAN, S. P. 1978 The ambipolarity paradox in toroidal diffusion, revisited. *Nucl. Fusion* **18** (7), 917.
- ITOH, K. & ITOH, S.-I. 1996 The role of the electric field in confinement. *Plasma Phys. Control. Fusion* **38** (1), 1.
- ITOH, K., ITOH, S.-I., DIAMOND, P. H., HAHM, T. S., FUJISAWA, A., TYNAN, G. R., YAGI, M. & NAGASHIMA, Y. 2006 Physics of zonal flows a. *Phys. Plasmas* **13** (5), 055502.
- KAGAN, G. & CATTO, P. J. 2008 Arbitrary poloidal gyroradius effects in tokamak pedestals and transport barriers. *Plasma Phys. Control. Fusion* **50** (8), 085010.
- KULSRUD, R. M. 1961 Hydromagnetic equilibria in a toroid from the particle point of view. *Phys. Fluids* **4** (3), 302–314.
- KULSRUD, R. M. 1980 *MHD Description of Plasma*. Princeton University.
- KUNZ, M. W., SCHEKOCIHIN, A. A., CHEN, C. H. K., ABEL, I. G. & COWLEY, S. C. 2015 Inertial-range kinetic turbulence in pressure-anisotropic astrophysical plasmas. *J. Plasma Phys.* **81** (5), doi:[10.1017/S0022377815000811](https://doi.org/10.1017/S0022377815000811).
- LANDREMAN, M. & CATTO, P. J. 2010 Effects of the radial electric field in a quasisymmetric stellarator. *Plasma Phys. Control. Fusion* **53** (1), 015004.
- MEDVEDEV, M. V., DIAMOND, P. H., ROSENBLUTH, M. N. & SHEVCHENKO, V. I. 1998 Asymptotic theory of nonlinear Landau damping and particle trapping in waves of finite amplitude. *Phys. Rev. Lett.* **81** (26), 5824.
- ROGERS, B. N., DORLAND, W. & KOTSCHENREUTHER, M. 2000 Generation and stability of zonal flows in ion-temperature-gradient mode turbulence. *Phys. Rev. Lett.* **85** (25), 5336.
- ROSENBLUTH, M. N. & HINTON, F. L. 1998 Poloidal flow driven by ion-temperature-gradient turbulence in tokamaks. *Phys. Rev. Lett.* **80** (4), 724.

- SUGAMA, H. & WATANABE, T.-H. 2006*a* Collisionless damping of geodesic acoustic modes. *J. Plasma Phys.* **72** (6), 825–828.
- SUGAMA, H. & WATANABE, T.-H. 2006*b* Collisionless damping of zonal flows in helical systems. *Phys. Plasmas* **13** (1), 012501.
- SUGAMA, H. & WATANABE, T.-H. 2009 Turbulence-driven zonal flows in helical systems with radial electric fields. *Phys. Plasmas* **16** (5), 056101.
- TERRY, P. W. 2000 Suppression of turbulence and transport by sheared flow. *Rev. Mod. Phys.* **72** (1), 109.
- WATANABE, T. H., SUGAMA, H. & NUNAMI, M. 2011 Effects of equilibrium-scale radial electric fields on zonal flows and turbulence in helical configurations. *Nucl. Fusion* **51** (12), 123003.
- XIAO, Y., CATTO, P. J. & MOLVIG, K. 2007 Collisional damping for ion temperature gradient mode driven zonal flow. *Phys. Plasmas* **14** (3), 032302.